# A method for characterizing the magnetic field response of a gradient system

**S. J. Vannesjö[1], M. Häberlin[1], L. Kasper[1], C. Barmet[1], and K. P. Pruessmann[1]**
[1]Institute for Biomedical Engineering, ETH and University Zürich, Zürich, Switzerland

**Introduction:** MRI relies on dynamic linear gradients for signal encoding. However the realization of given gradient time-courses is usually imperfect due to physical limitations, including limited bandwidth of gradient amplifiers, gradient chain delays, crosstalk between gradient coils, and eddy currents in the rest of the setup. Jointly, all of these mechanisms influence how the effective magnetic field dynamics in the magnet bore deviate from an ideal gradient response. The aim of the present work was to characterize this effective field response comprehensively based on actual field measurements. The resulting method is based on driving the gradient system with test pulses and measuring the resulting field dynamics with a third-order NMR camera.

**Methods:** Within the scope of this work an MRI scanner's gradient system is treated as one linear time-invariant system (LTI) with an input for each of three gradient chains and 16 outputs representing resulting field components up to third order in spherical harmonics (Tab. 1). Such a system can be fully described by 3 x 16 = 48 impulse response functions (IRF) [1,2], which translate the input functions $i_l(t)$ into the outputs $g_m(t)$ according to $g_m(t) = \sum_l \int i_l(\tau) \cdot irf_{l,m}(t-\tau) d\tau$ in time domain, $G_m(\omega) = \sum_l I_l(\omega) \cdot IRF_{l,m}(\omega)$ in frequency domain, giving rise to the net magnetic field $B(\mathbf{r},t) = \sum_m b_m(\mathbf{r}) \cdot g_m(t)$. Field responses were measured with a field camera consisting of 16 NMR probes distributed on a 20-cm sphere [3], allowing to extract dynamic phase coefficients $k_m(t) = \gamma \int_0^t g_m(\tau) d\tau$. In this representation (cf. Tab. 1), $k_0$ is a global phase term reflecting potential dynamics of $B_0$, $k_{1\text{-}3}$ correspond to the conventional $k_x$, $k_y$, $k_z$, and $k_{4\text{-}8}$ and $k_{9\text{-}15}$ describe 2nd- and 3rd-order terms respectively [4]. The corresponding $g_m(t)$ were obtained by differentiation of $k_m(t)$. Measurements were performed on 3T and 7T Philips Achieva systems (Philips Healthcare, Best, NL / Cleveland, USA). Per gradient channel six triangular gradient blips of different duration [0.20-0.33 ms; peak amplitude 18 and 12 mT/m at 3T and 7T respectively] were applied as test inputs. The variation in blip duration served to compensate for zeros in individual blip spectra and was chosen such as to cover the gradient systems' expected bandwidth. The desired IRFs were obtained by deconvolution of $g_m(t)$ in the Fourier domain using least-squares fitting to combine data obtained with different blip lengths. For validation the resulting IRFs were used to predict the actual field dynamics of various other gradient waveforms.

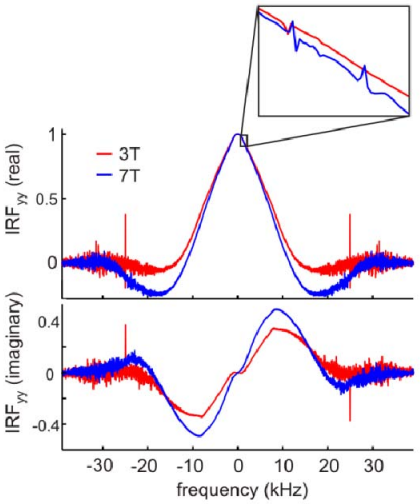


*Fig 1: Measured IRF in y-direction at 3T and 7T*

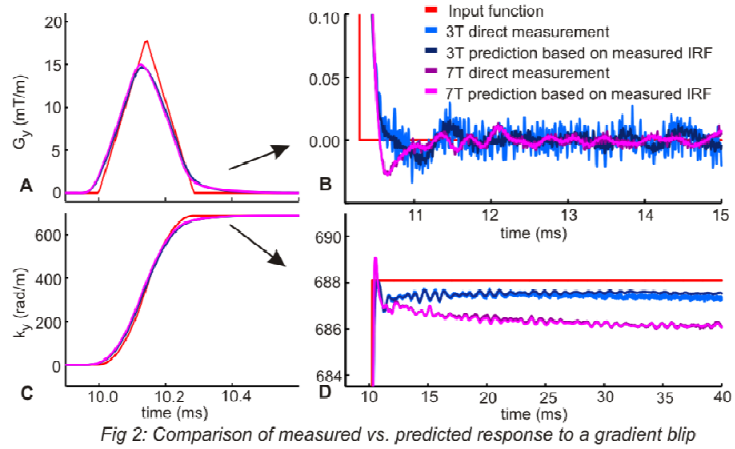


*Fig 2: Comparison of measured vs. predicted response to a gradient blip*

**Tab.1: spherical harmonics**

| nr. | basis function $b_m$ |
|---|---|
| 0 | 1 |
| 1 | x |
| 2 | y |
| 3 | z |
| 4 | xy |
| 5 | zy |
| 6 | $3z^2 - (x^2+y^2+z^2)$ |
| 7 | xz |
| 8 | $x^2 - y^2$ |
| 9 | $3x^2y - y^3$ |
| 10 | xyz |
| 11 | $y(5z^2 - (x^2+y^2+z^2))$ |
| 12 | $5z^3 - 3z(x^2+y^2+z^2)$ |
| 13 | $x(5z^2 - (x^2+y^2+z^2))$ |
| 14 | $x^2z - y^2z$ |
| 15 | $x^3 - 3xy^2$ |

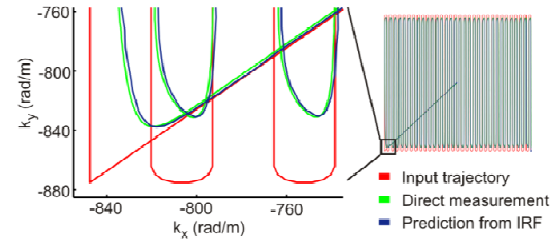


*Fig 3: Predicted vs. measured trajectory of an EPI*

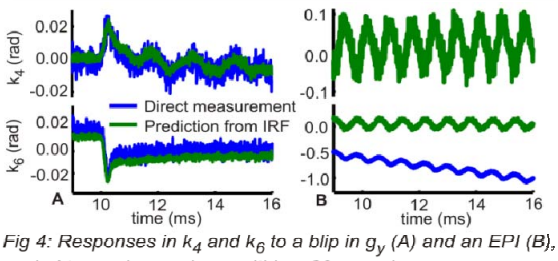


*Fig 4: Responses in $k_4$ and $k_6$ to a blip in $g_y$ (A) and an EPI (B), scaled to maximum phase within a 20 cm sphere*

**Results:** The study focused on the first-order IRFs, i.e., on the desired gradient responses. Their bandwidths at FWHM were approximately 19 kHz at 7T and 17 kHz at 3T. Figure 1 shows the real and imaginary part of the first-order IRF in the y-direction, at both field strengths. In the central part of the IRF (within ±3000 Hz) a pattern of very small peaks was found, specific to each gradient direction, that correspond to mechanical vibrations of the gradient coils (Fig. 1, top). In the time domain the effects of the mechanical vibrations are seen as oscillations in the k-coefficient after the end of a gradient pulse (Fig 2D). The oscillations are reproducible and can be predicted with very high accuracy over a wide range of pulse shapes and sizes. Triangular and trapezoidal gradient pulse shapes of 0.2-25 ms length and 0.1–40 mT/m amplitude, were well predicted by the IRF. Figure 2 shows the response of the gradient system to a short triangular pulse, showing the smoother shape of the actually performed gradient. The total area of the pulse, as reflected in the step size of the k-trajectory, was conserved (Fig. 2C-D), with a prediction error of ~0.1%. The prediction stayed within the same error range for longer sequences with high-amplitude gradient pulses, such as EPI (Fig. 3). A predictable effect of the gradients could also be seen in $k_0$, as well as in the higher-order coefficients (Fig. 4). However, the higher-order responses were generally small, making their exact prediction difficult in the presence of thermal drifts, non-linearities of the gradient response and measurement noise.

**Conclusion:** The impulse response of gradient systems can be determined with great accuracy by measuring the responses to a suitable set of test inputs with an NMR field camera. The procedure is simple and fast and permits the reliable prediction of actual k-space trajectories as well as of reproducible higher-order effects. It could serve as the basis of system optimization through pre-emphasis adjustments and for improved image reconstruction.

**References:**

[1] Alley, Glover and Pelc, 1998 Magn. Res. Med 39:581-7.
[2] Addy, Wu and Nishimura, 2009 Proc. ISMRM, p3068.
[3] Barmet, Wilm, Pavan and Pruessmann, 2009 Proc. ISMRM, p780.
[4] Barmet, De Zanche and Pruessmann, 2008 Magn. Res. Med 60:187-197.